Magnetic fields of the optical matching devices used in the positron source of the ILC

Richard Pausch
Dresden University of Technology
DESY Summer Students Programme 2010

Supervisors: Andreas Schälicke, Andriy Ushakov
DESY Zeuthen

Abstract

This report summarizes the study of the magnetic flux densities for two different optical matching devices (OMD) proposed for the positron source of the International Linear Collider (ILC). The goal of this study was to simulate the magnetic fields of the various OMDs and to find a way to include the results in a beamline simulation of the positron source.

1 The International Linear Collider

1.1 Introduction

The *International Linear Collider* (ILC) is a proposed counterpart to the LHC, analyzing its results in more detail. In contrast to the LHC, the ILC will be a linear collider. It is anticipated to collide polarized electrons with polarized positrons. By using e^+e^--collisions, one will be able to reconstruct the events more easily and thus being able to measure the properties of particles and their interactions more accurately. The polarization offers the advantage, that one can suppress certain particle interactions and increase the effective luminosity for interactions one is interested in. An example of using polarized beams is that one would be able to distinguish potential super symmetric particles or other predicted particles beyond the standard model. [1]

1.2 The positron source

As mentioned before, the ILC uses polarized positrons. To produce them, high energetic electrons from the main electron linear accelerator are sent through a helical undulator (see figure 1). After that, they are returned to the main electron linac by using a bending magnet. While going through the undulator, the electrons radiate circular polarized photons. The photons hit a rotating metal target. There, the photons interact with atoms and can produce particle showers. As part of those showers, longitudinally polarized electrons and positrons are created via pair production (see figure 2). To increase the average polarization of the positrons, a photon-collimator is used.
To optimize the positron yield an apparatus called *optical matching device* (OMD) creates a

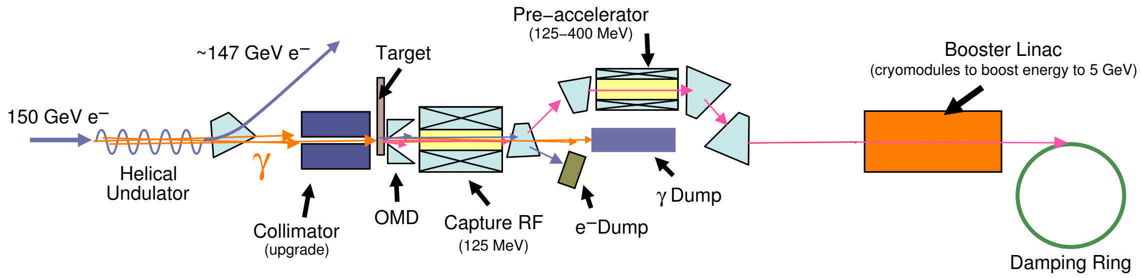

Figure 1: Schematic drawing of the ILC's positron source [2]

tapering magnetic field, so that the positrons do not leave to the side but circle around the central beam line. Right now, there are three different proposals for that device. After the OMD, the positrons are separated from the electrons by a magnet. The produced electrons are dumped just as the photons, which did not interact. The positrons are directed to a pre-accelerator and a booster linac to increase their energy and then are stored in a damping ring till they are used for the collisions in the main linear accelerator.

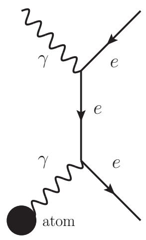

Figure 2: Feynman diagram of pair production

2 Work at DESY Zeuthen

In Zeuthen, several people are working on the development of the ILC. In particular, one group is working on simulations of the positron source. For that, they developed a software called *PPS-SIM* [3].

2.1 PPS-SIM-Software

The PPS-SIM-Software is based on *Geant4* and *ROOT* and is able to simulate the positron source from the undulator up to the first accelerator structures. PPS-SIM supports different proposals and includes the ability to change several parameters of the source. It also comprises a graphical user interface, so that people not familiar with ROOT, Geant4 or C++ are able to use this software, and a batch mode enabling high statistics runs.
PPS-SIM is able to simulate all three proposed OMDs: the *quarter wave transformer* (QWT), the *adiabatic matching device* (AMD) and the *lithium lens*. To model the effects of the OMDs on the particle beam, the magnetic fields of the OMDs are described by using simplified

functions. To include more realistic fields in PPS-SIM, the magnetic flux densities needed to be simulated.

2.2 Methods used

To simulate the magnetic flux densities caused by the QWT and the AMD, Maxwell's equations needed to be solved including all boundary conditions and material properties. To do this, a software called *FlexPDE* was used. It enables the user to describe the geometry, enter material properties and defining the partial differential equations to be solved by using a simple script language. On this basis, the software creates a grid and solves the given equations using the finite element method. The results are returned for single points of the grid. However, this discrete data can not be implemented directly for the simulation in PPS-SIM. One has to find a continuous function describing the data which then can be used in PPS-SIM.

3 Magnetic fields of the QWT

The *quarter wave transformer* (QWT) is one of the possible OMD's used for the ILC.

3.1 Design of the QWT

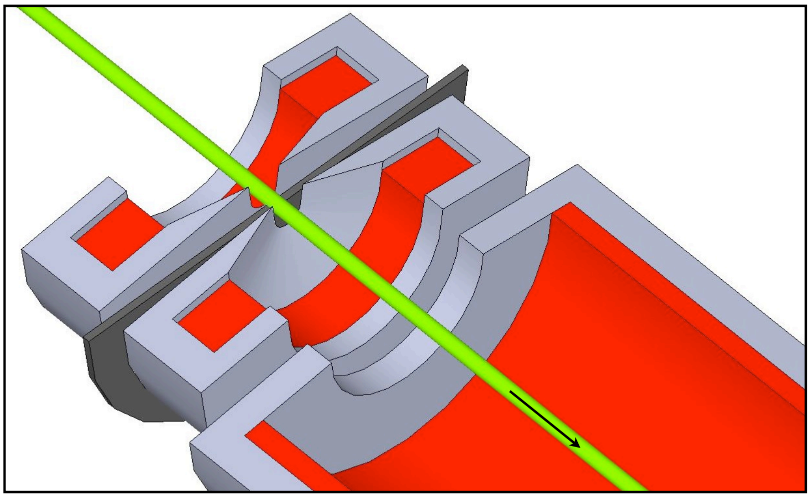

Figure 3: Cut through the QWT

The basic design of the quarter wave transformer is shown in figure 3. It is cut in half so that all parts are properly visible. The green line going through the center is representing the main beamline with the beam going from the upper left to the lower right corner. The dark grey part is the target. Because it is under constant stress caused by the incoming photons, it is planned to spin the target to prevent its destruction. For simplification, the apparatus doing that is not drawn here. Surrounding the target, there are two solenoids. Both consist of copper coils with an the electric current, drawn in red, and an iron shielding to reduce eddy currents at the target, drawn in light grey. The currents in both coils have the same magnitude but flow in different directions. Downstream, the radio frequency cavity is located.

Again, the light grey part is the surrounding iron and the red part is the current flowing in a copper coil.
For future references, the origin of the coordinate system is the center of the target. The z-axis is equivalent to the beam line and ρ will be the perpendicular distance between the z-axis and the point of interest as in any cylindrical coordinates system.

3.2 Relations from symmetry

In general, the magnetic vector potential $\vec{A}$ can be calculated by to following equation:

$$\vec{A}(\vec{r}) = \int \mathrm{d}^3\mathrm{r'}\, \frac{\vec{j}(\vec{r'})}{|\vec{r} - \vec{r'}|} \tag{1}$$

First of all, one can easily see, that $\vec{A}$ is constant on the axis of rotation and because there is a gauge freedom we can set the value of $\vec{A}$ on the axis to zero.
In a first order approximation, the current through the solenoid can be regarded as to have just components in $\vec{e}_\varphi$ direction. Thus, the components A_ρ and A_z of the vector potential, considering our first gauging, are zero. The vector potential is simplified to:

$$\vec{A} = (0, A_\varphi, 0) \tag{2}$$

3.3 Simulation of the magnetic field and vector potential

From Maxwell's equations we know, that if there is no time depending electrical field $\vec{E}$, then $\vec{\nabla} \times \vec{B} = \mu_r \mu_0 \vec{j}$. The relation between vector potential and magnetic flux density is given by $\vec{\nabla} \times \vec{A} = \vec{B}$. The function to solve is therefore:

$$\vec{\nabla} \times \left(\vec{\nabla} \times \frac{\vec{A}}{\mu_0 \cdot \mu_r} \right) = \vec{j} \tag{3}$$

This equation was entered in FlexPDE together with all necessary boundary conditions and material properties. The results of the vector potential and the non-zero components of the magnetic field were exported as data files and stored for future use.

3.4 Fitting the results for future use in PPS-SIM

3.4.1 Mathematical background

The data received from FlexPDE is discrete but for the simulation of the beamline a continues field is needed. To achieve that, a solution to Maxwell's equation had to be chosen, to fit the simulated data onto this solution. In this case, the spherical harmonics Y_l^m seemed to be a good choice.

$$Y_l^m = (-1)^m \left[\frac{2l+1}{4\pi} \frac{(l-m)!}{(l+m)!} \right]^{1/2} P_l^m(\cos\theta)\, \mathrm{e}^{im\phi} \quad \text{spherical harmonics} \tag{4}$$

$$P_l^m(x) = 2^{-l} \sum_{m=0}^{l/2} (-1)^m \binom{l}{m} \binom{2l-2m}{l} x^{l-2m} \quad \text{Legendre polynomials} \tag{5}$$

$$\psi(r,\theta,\phi) = \sum_{l=0}^{\infty} \sum_{m=-l}^{l} Y_l^m(\theta,\phi) \cdot \left[a_{lm} \cdot r^l + b_{lm} \cdot r^{-(l+1)} \right] \tag{6}$$

The scalar function ψ automatically fulfills the Laplace equation $\vec{\nabla}^2\psi(r,\theta,\phi) = 0$ and because the Gauss's law for magnetism states that $\vec{\nabla}\cdot\vec{B} = 0$, the function $\psi(r,\theta,\phi)$ can be used to describe the magnetic flux density $\vec{B}$. The relation between them is therefore given by:

$$\vec{B} = \vec{\nabla}\psi(r,\theta,\phi) \tag{7}$$

Because of the QWT's rotational symmetry it is possible to consider just spherical harmonics with $m = 0$. For further simplification, all constant factors depending only on l were excluded from the implemented equations (for further details see below).

3.4.2 Software implementation

With the discrete data from the simulation at hand, the spherical harmonics needed to be fitted to this data. This was done using the programming language *Python* and the library *minuit2* provided by *ROOT*. To describe the deviation between fitted function and simulated values, a χ^2-function was defined as follows:

$$\chi^2 = \sum_{\text{data}} \left(\hat{B}_z(\rho,z) - B_z(\rho,z)\right)^2 \tag{8}$$

In this formula, $\hat{B}_z$ are the simulated values for the magnetic flux density in z-direction coming from FlexPDE. Here, only data from a small region of interest, starting at the target and going to the RF-cavity, was used. B_z is the z-component of the magnetic induction calculated using (7). If the scalar potential ψ is described by the spherical harmonics, then the components of the magnetic flux density have to be calculated as described below. Before, it should be mentioned that the functions below are those implemented in the fitting algorithm. Some constant factors from the spherical harmonics were included in the fitting parameters and thus do not appear in the function. This has to be considered if implementing the results in an other software.

Additionally a point of origin for the spherical harmonics had to be chosen. The natural point would be the crossing point of the target and the photon beam. However, at this point $r = 0$, which would require all b_{lm} elements to be zero; otherwise there would be a divergence at the point of origin. Hence, an offset from this point was introduced. The point of origin was placed at $(\rho = 0, z = -o)$ and the following definitions were established:

$$\mu = \frac{z+o}{r} \tag{9}$$

$$r = \sqrt{(z+o)^2 + \rho^2} \tag{10}$$

In the implemented algorithm, the sum in equation 6 was broken apart and all exponents were dealt with separately. Thus, the exponent $p(i)$ was introduced and all fields could be described as follows:

$$f(r,\theta,\phi) = \sum_i P_{l(i)}(\mu)\cdot a_i \cdot r^{p(i)} \tag{11}$$

$$B_z = \frac{\partial f(r,\theta,\phi)}{\partial z} = \sum_i a_i \cdot r^{p(i)-1}\left[P'_{l(i)}(\mu)\cdot\left\{1-\mu^2\right\} + P_{l(i)}(\mu)\cdot p(i)\cdot\mu\right] \tag{12}$$

$$B_\rho = \frac{\partial f(r,\theta,\phi)}{\partial \rho} = \sum_i a_i \cdot \rho \cdot r^{p(i)-2}\left\{-P'_{l(i)}(\mu)\cdot\mu + P_{l(i)}(\mu)\cdot p(i)\right\} \tag{13}$$

These formulae are implemented in the python program. The parameter for $p(i) = 0$ has been excluded from the fit because it does not contribute to the magnetic flux density and therefore causes an error in the minuit2 algorithm.
If the position of the offset o is also set as an optimizable parameter, minuit2 is again not able to finish the fit because there seems to be a variety of local minima. To avoid this problem, the offset was fixed before handed over to minuit2. This was done for several offsets and the results are given in figure 4. Because this was a serious calculation, the *batch farm* was used to obtain results in an acceptable time.
The results from this calculation revealed, that there really are several local minima and that χ^2 is extremely sensitive to the actual value of the offset (see inner diagram of figure 4). For example, a $\Delta o \sim 10^{-16}$ m difference in the offset can cause a discrepancy of up to $\Delta\chi^2 \sim 0{,}01$ using the minuit2 algorithm. Realizing that, it is clear that fitting the offset using minuit2 alone produced errors in most cases, because the minuit2 algorithm uses, among others, the partial derivative of χ^2 with respect to the offset, which is not calculable for this function. Looking at the results in figure 4, the best choice for an offset lies around $o = 0{,}4245$ m

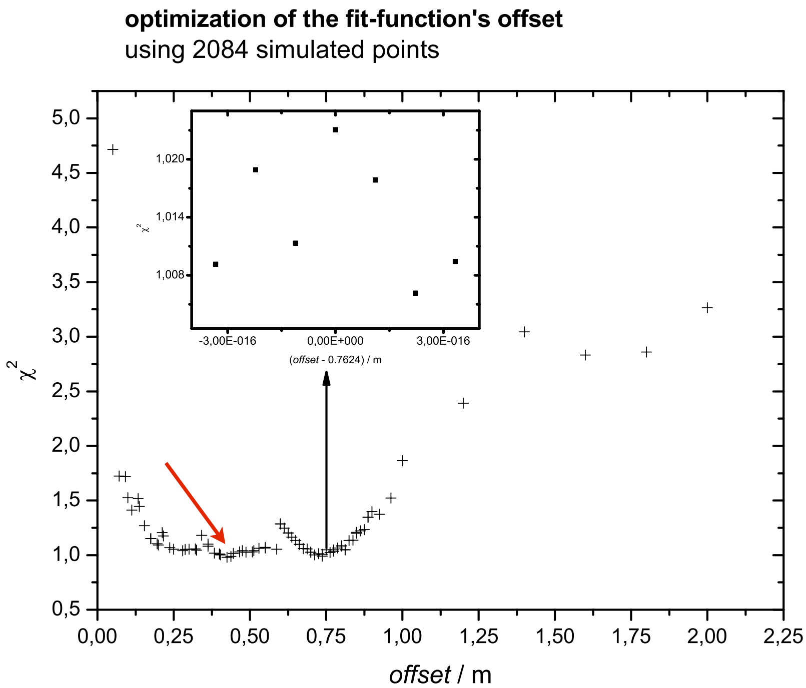

Figure 4: χ^2 over the offset and a detailed look at $o = 0{,}7624$ m

(marked with a red arrow). Additionally 37 other parameters a_i, about half of them with positive $p(i)$ and the other half with negative exponents, were used to describe the scalar function f. This number of parameters allowed a relative error of the magnetic induction of less than 10% in an area close to the main beamline.
However, all those parameters describe the magnetic field only for a maximum of 1 T. To optimize the positron source, a possibility to change the maximum flux density without having to go through all previous steps again, would be beneficial. To check, if it is possible to describe the parameters a_i for different currents in the first solenoid, the entire procedure was repeated

for several different current densities. However, the offset was held constant because of the known problems discussed above. It turned out that for using a total of 37 parameters, the relationship between current density and parameters was nearly linear. For less parameters, this seemed not to be the case. Hence, a linear approximation for describing the parameter values was used for the 37 parameters:

$$a_i = A_i \cdot i_{\text{sol}} + B_i \tag{14}$$

In this equation a_i is the parameter of the spherical harmonics with summation-index i, A_i and B_i are parameters for the linear function describing the linear fit. i_{sol} is the current density in the first solenoid.
For magnetic flux densities below 1,0 T the behavior was not linear anymore, so that the calculated parameters can only be used in a range of 1,0 T to 2,5 T. To check the accuracy of this method, the results using the calculated parameters were compared to newly simulated data from FlexPDE. For all checked currents, the spherical harmonics described the simulated data adequate enough (see figure 5).

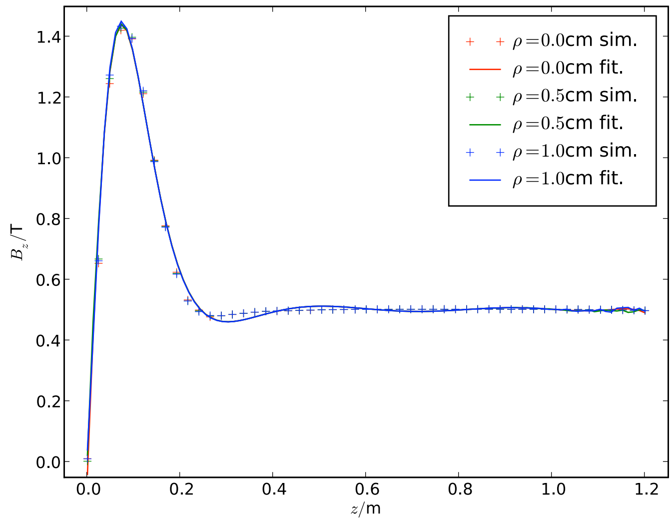

Figure 5: Simulated and calculated data for a maximum of $B_z = 1{,}4\,\text{T}$

4 Magnetic fields of the AMD

4.1 Design of the AMD

The AMD consists of a series of copper coils and so called magnetic shaping plates. There is a total of five current-carrying copper coils and six shaping plates. The coils are simple cylinders with a hole in the middle. The shaping plates are also made out of copper, but they are not perfectly cylindrical. All of them are cut to minimize eddy currents and the cut of two adjacent plates form an angle of 60°.
Figure 6 shows just one half of the first two shaping plates (grey and blue) and the copper coil (green) in between. The yellow cylinder in the middle is supposed to represent the main beamline with photons coming from the bottom, hitting a target, not drawn here, directly in

front of the AMD and finally passing the AMD through the first hole. For simplification, not all surfaces are transparent but some are completely clear. The cuts are drawn in red.
For the three dimensional simulation using FlexPDE, just these three parts of the AMD shown here were used, because this was supposed to be used as a first test.

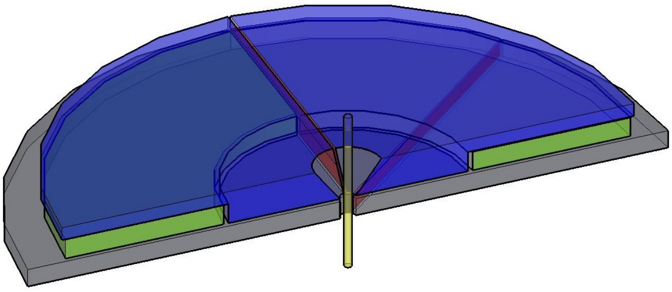

Figure 6: Cut through part of the AMD

The currents through the coils is reducing with the distance to the target. This causes the magnetic induction in z-direction to have a maximum near the first two shaping plates. By using pulsed currents, a current is induced in the shaping plates. This is supposed to increase the magnetic field in the center as described in [4].

4.2 Problems with FlexPDE

Because the design of the AMD has no rotational symmetry, a three dimensional approach to describe the device was needed. However, to get a basic understanding of the physics behind the AMD, rotational symmetry was assumed and based on that, a first model was created.
Including the three dimensional model turned out to be a challenge on its own. Several approaches were taken to include the AMD's geometry in FlexPDE. In most cases, the approach could not be used, because of internal errors in FlexPDE. Under the most common ones were: creating a mesh with a depth of nearly zero, where no grid should be; missing grid points close to the cuts or the number of cells running off for thin layers. Most of these problems had to do with the sloped holes in the middle of the shaping plates.

4.3 Mathematical background

Because simulating the magnetic flux density of the AMD is a time depending problem, equation 3 has to be adjusted. From Maxwell's equation, we know, that:

$$\vec{\nabla} \times \vec{B} = \mu_0 \mu_r \left(\vec{j} + \vec{j}_{\text{ind.}} \right) + \mu_0 \mu_r \cdot \varepsilon_0 \varepsilon_r \cdot \frac{\partial \vec{E}}{\partial t} \tag{15}$$

Because there are no free charged particles, the electric field can be described by $\vec{E} = -\frac{\partial \vec{A}}{\partial t}$. The induced current is given by $\vec{j}_{\text{ind.}} = \sigma \cdot \vec{E}$, with σ being the conductance. By combining all equations one gets a partial differential equation of second order in time:

$$\vec{\nabla} \times \left(\frac{\vec{\nabla} \times \vec{A}}{\mu_0 \mu_r} \right) = \vec{j} - \sigma \cdot \frac{\partial \vec{A}}{\partial t} - \varepsilon_0 \varepsilon_r \cdot \frac{\partial^2 \vec{A}}{\partial t^2} \tag{16}$$

This formula was implemented in FlexPDE, excluding the last term, because its contribution was very small.

4.4 Results from the simulations

As mentioned, the current through the coils is time dependent to increase the flux density and this time dependency was considered in both the two dimensional and the three dimensional simulation.

4.4.1 2D-simulation

For the two dimensional simulation, an additional condition was introduced for the induced currents to compensate for the missing cuts in the shaping plates. This was realized by demanding that the total induced current on the cut-section had to be zero. This prevented the induced currents from circling the shaping plates in just one direction. As expected, a current close to the copper coils was induced and caused an compensating current closer to the beamline. However, for the time dependent simulation, the magnetic flux density was still by three orders of magnitude lower than expected.

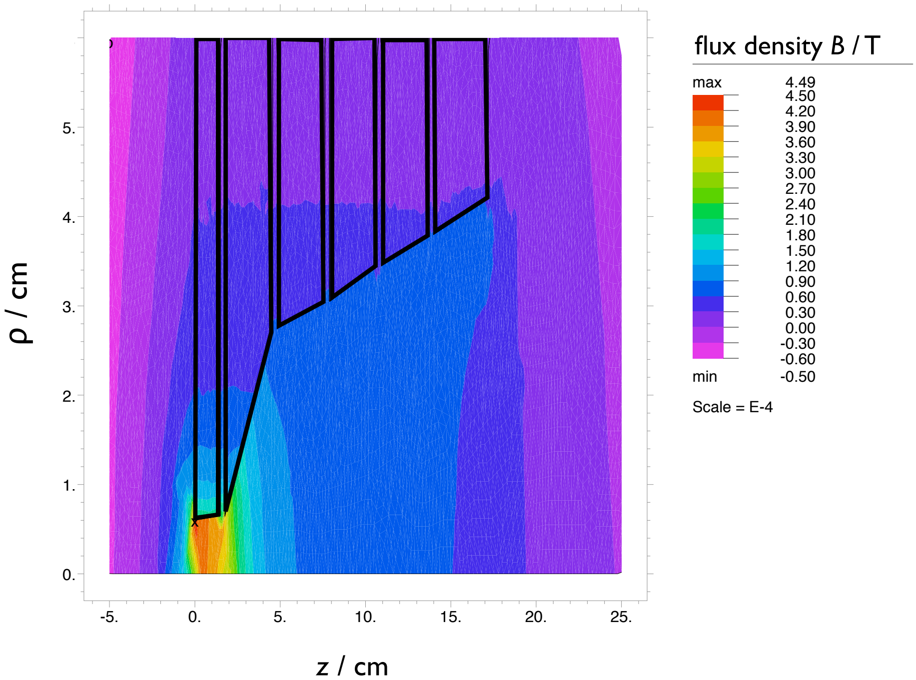

Figure 7: Magnetic flux density - 2D simulation

4.4.2 3D-simulation

A working 3D-model of the first parts of the AMD was created, which demonstrates how to include further parts in FlexPDE. All expected physical effects could be simulated qualitatively. The obtained results show obvious discrepancies and further checks are needed.

5 Conclusions

5.1 The quarter wave transformer

A possible way of including realistic magnetic fields for the QWT has been shown. The only task left is to include this in PPS-SIM. For that, the scalar function and its derivatives have to be written in C++ code to replace the simplified functions describing the magnetic field at the moment.

5.2 The adiabatic matching device

The basic functionality of the AMD could be reproduced. However, because of the different results in the magnitude of the magnetic fields compared to the data from LLNL [4], it was not attempted to include the simulated magnetic fields in PPS-SIM. Further investigations need to be done, to fully understand the physical behavior of this device.

Acknowledgements

I would like to thank DESY for offering this unique summer school. The work and the offered lectures have been wonderful. Special thanks go to my supervisors Andreas Schälicke and Andriy Ushakov for their patience and support. Thank you for all the nice discussions. Thanks also to Sabine Riemann, who supported my request of taking exams during the summer school. I would also like to thank Prof. Kobel and Prof. Zuber from Dresden University of Technology for supporting my application for the DESY summer school. And of course, thanks to all the other summer students who made this time unforgettable.

References

[1] G. A. Moortgat-Pick *et al.*
The role of polarized positrons and electrons in revealing fundamental interactions at the linear collider
Phys. Rept. **460** (2008) 131 [arXiv:hep-ph/0507011]

[2] Editors: Nan Phinney, Nobukasu Toge, Nicholas Walker
International linear collider reference design report
Volume 3: accelerator
August, 2007

[3] A. Ushakov, S. Riemann, A. Schälicke
Positron source simulations using Geant4
Proceedings of the 1st International Particle Accelerator Conference (IPAC'10)
Kyoto, Japan, 23-28 May 2010, 4095

[4] Tom Piggott, Jeff Gronberg
LLNL Update (flux concentrator, rotation vacuum seals)
7$^{\text{th}}$ Positron Source Collaboration Meeting
Hamburg, Germany, 15-16 July 2010